Analysis, Design, and Optimization of InGaP–GaAs HBT Matched-Impedance Wide-Band Amplifiers With Multiple Feedback Loops

Ming-Chou Chiang, Shey-Shi Lu, *Senior Member, IEEE*, Chin-Chun Meng, Shih-An Yu, Shih-Cheng Yang, and Yi-Jen Chan

***Abstract*—The realization of matched impedance wide-band amplifiers fabricated by InGaP–GaAs heterojunction bipolar transistor (HBT) process is reported. The technique of multiple feedback loops was used to achieve terminal impedance matching and wide bandwidth simultaneously. The experimental results showed that a small signal gain of 16 dB and a 3-dB bandwidth of 11.6 GHz with in-band input/output return loss less than −10 dB were obtained. These values agreed well with those predicted from the analytic expressions that we derived for voltage gain, transimpedance gain, bandwidth, and input and output impedances. A general method for the determination of frequency responses of input/output return losses (or S_{11}, S_{22}) from the poles of voltage gain was proposed. The intrinsic overdamped characteristic of this amplifier was proved and emitter capacitive peaking was used to remedy this problem. The tradeoff between the input impedance matching and bandwidth was also found.**

***Index Terms*—InGaP–GaAs, multiple feedback, transimpedance amplifier, wideband.**

I. Introduction

WIDE-BAND amplifiers are used in variety of modern electronic systems such as microwave/lightwave communication and instrumentation [1]. Among the many versions of wide-band amplifiers, the so-called Kukielka configuration [2] is one of the popular circuits. It has been fabricated by silicon bipolar, AlGaAs–GaAs heterojunction bipolar transistor (HBT), and InAlAs–InGaAs HBT processes with excellent performance [3]–[5]. Recently, InGaP–GaAs HBT technology has attracted much attention because of its uniformity [6]–[9] and reliability [10]. However, no detailed account of the performance of the InGaP HBT wide-band amplifiers with Kukielka configuration has been reported in the literature. The design equations based *directly* on the Kukielka configuration also have not been given before.

Manuscript received July 9, 2001; revised March 3, 2002. This work was supported by the National Science Council and Ministry of Education, Taiwan, R.O.C., under Grant NSC90-2219-E002-009, Grant NSC90-2219-E005-001, and Grant 89-E-FA-06-2-4.

M.-C. Chiang, S.-S. Lu and S.-A. Yu are with the Department of Electrical Engineering and Graduate Institute of Electronics, National Taiwan University, Taipei, Taiwan, R.O.C. (e-mail: sslu@cc.ee.ntu.edu.tw).

C.-C. Meng is with the Department of Electrical Engineering, National Chung-Hsing University, Taichung, Taiwan, R.O.C (e-mail: ccmeng@nchu.edu.tw).

S.-C. Yang and Y.-J. Chan are with the Department of Electrical Engineering, National Central University, Chung-Li, Taiwan, R.O.C. (e-mail: yjchan@ee.ncu.edu.tw).

Publisher Item Identifier S 0018-9200(02)04935-1.

Therefore, in this paper, we present the first demonstration of Kukielka wide-band amplifiers using InGaP–GaAs HBT process. Multiple feedback loops were used to achieve terminal impedance matching and wide bandwidth simultaneously. The capacitive peaking technique [11] was used to overcome the intrinsic overdamped frequency response of the Kukielka amplifiers and thus enhance the bandwidth. The experimental results showed that a small signal gain of 16 dB and a 3-dB bandwidth of 11.6 GHz with in-band input/output return loss less than −10 dB were achieved. These values were in good agreement with the values predicted by the analytic expressions that we derived for voltage gain, bandwidth, and input and output impedances. A method to calculate the frequency responses of input/output return losses based on the poles of voltage gain is also presented.

II. Principles of Circuit Design

The circuit topology of the Kukielka wide-band amplifier is shown in Fig. 1(a). The input stage consists of a single transistor Q_1 driving the output stage consisting of a transistor Q_2 with local shunt (R_{f2}) and series (R_{e2}) feedback. There is also an overall shunt-series feedback loop composed of resistors R_{e2} and R_{f1}. Local shunt feedback around Q_2 gives a low impedance at the collector node of Q_2 for the output terminal impedance matching. Then, global shunt feedback is applied around this voltage amplifier via R_{f1} to achieve the input matching condition. Clearly, this amplifier can be approximated by a two-pole system with the closed-loop poles determined by the following characteristic equation:

$$s^2 + s(\omega_{p1} + \omega_{p2}) + (1 + A_O\beta)\omega_{p1}\omega_{p2} = 0 \qquad (1)$$

where A_O is open-loop gain at low frequencies, β is the feedback factor, and ω_{p1} and ω_{p2} are the two poles of the A circuit. Thus, the closed-loop poles P_1 and P_2 are given by

$$P_1, P_2 = -\frac{1}{2}(\omega_{p1} + \omega_{p2}) \pm \frac{1}{2}\sqrt{(\omega_{p1} + \omega_{p2})^2 - 4(1 + A_O\beta)\omega_{p1}\omega_{p2}}. \qquad (2)$$

From this equation, we see that as the loop gain $T = A_O\beta$ is increased from zero, the poles are brought closer together. Then a value of loop gain is reached at which the poles become coincident. If the loop gain is further increased, the poles become

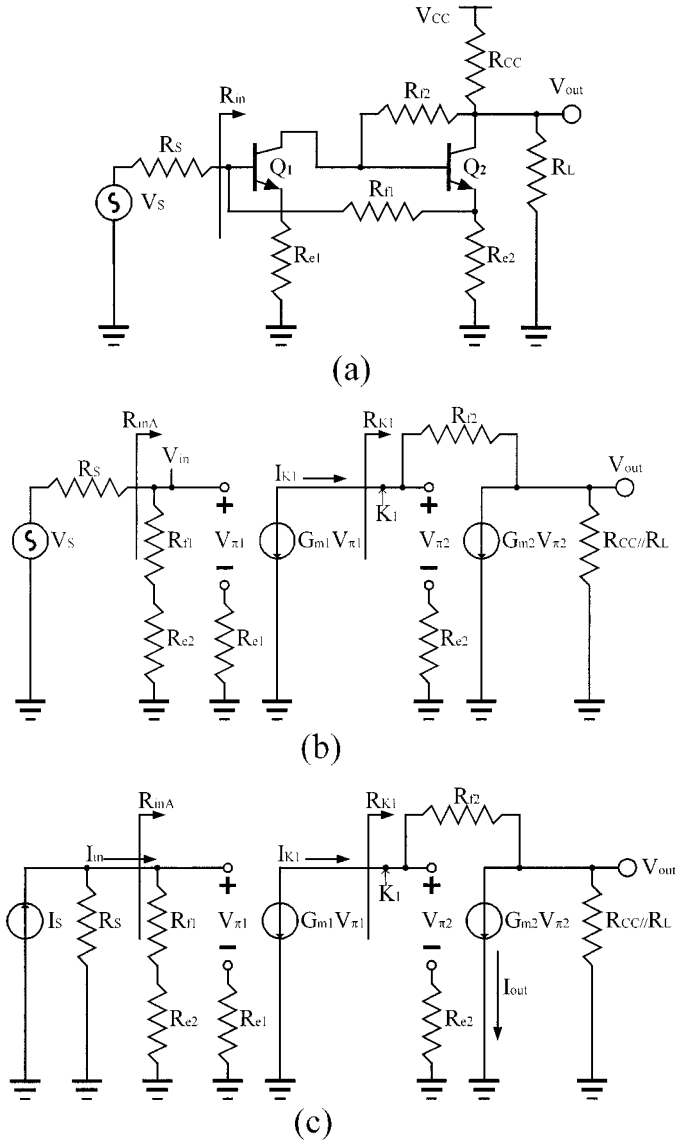

Fig. 1. The ac schematics of the Kukielka amplifier. (a) Basic topology. (b) The A circuit of (a) for calculating voltage gain. (c) The A circuit of (a) for calculating current gain.

complex conjugate. The characteristic (1) can also be written in the standard form

$$s^2 + s\frac{\omega_0}{Q} + \omega_0^2 = 0 \tag{3}$$

where $\omega_0 = [(1 + A_O\beta)(\omega_{p1}{}^*\omega_{p2})]^{1/2}$, $Q = [(1 + A_O\beta)\omega_{p1}\omega_{p2}]^{1/2}/(\omega_{p1} + \omega_{p2})$. A value of $Q = 0.707$ results in the maximally flat response with a bandwidth of ω_0. If ω_{p1} is initially equal to ω_{p2}, then a loop gain of $A_O\beta = 1$ is required to achieve the maximally flat response.

From the above description, we may summarize the design procedure of the Kukielka amplifier as follows. First, decide the required voltage gain. Then, bring the two poles to be equal by R_{e1} and R_{f2}. Finally, adjust R_{e2} and R_{f1} for the output impedance and input impedance matching, respectively. In order to go through the above-mentioned design procedure, the formulas for poles, voltage gain, current gain, loop gain, and input and output resistances have to be found. These derivations are given in the following.

A. Positions of Poles

Careful analysis of the circuit (in the absence of global feedback) [2], [13] yields approximate pole positions given by

$$\omega_{P1} \approx \frac{g_{m1}}{\dfrac{C_{\pi 1} \times g_{m1}}{1 + g_{m1} \times R_{e1}} \times [(R_s + r_{b1} + R_{e1}) || (R_{f1} + R_{e2})]} \approx \frac{\omega_{T1}}{G_{m1} \times R_s} \tag{4a}$$

$$\omega_{P2} \approx \frac{g_{m2}}{\dfrac{g_{m2} \times C_{\pi 2}}{1 + g_{m2} \times R_{e2}} \times \left[\dfrac{R_{f2} + (R_{cc} // R_L)}{1 + G_{m2} \times (R_{cc} // R_L)} + r_{b2} + R_{e2}\right]} \approx \frac{\omega_{T2}}{R_{f2}} \times (R_{cc} // R_L) \tag{4b}$$

where $C_{\pi 1}$ and $C_{\pi 2}$ are base–emitter junction capacitances of Q_1 and Q_2, r_{b1} and r_{b2} are the spreading base resistances of Q_1 and Q_2, g_{m1} and g_{m2} are the transconductances of Q_1 and Q_2,; $G_{m1}(= g_{m1}/(1 + g_{m1}R_{e1}))$ and $G_{m2}(= g_{m2}/(1 + g_{m2}R_{e2}))$ are the effective transconductances of Q_1 and Q_2, and ω_{T1} and ω_{T2} are the cutoff frequencies of Q_1 and Q_2, respectively. Clearly, the two poles can be brought to be coincident by choosing suitable G_{m1} (i.e., R_{e1}) and R_{f2}.

B. Current and Voltage Gains

In order to calculate the current gain and voltage gain, two representations of the A circuit for the Kukielka amplifier *without* the global shunt-series feedback is shown in Fig. 1(b) and (c). In Fig. 1(b), the impedance at point K_1 looking into the base of Q_2 is given by

$$R_{K1} = \frac{R_{f2} + R_{cc} // R_L}{1 + G_{m2} \times (R_{cc} // R_L)}. \tag{5a}$$

Therefore, the voltage gain of $V_{\text{out}}/V_{\text{in}}$ *without* global feedback is

$$A_V = \frac{V_{\text{out}}}{V_{\text{in}}} \approx G_{m1} R_{K1} G_{m2} (R_{f2} // R_{cc} // R_L) \approx G_{m1} R_{f2} \left(1 - \frac{R_{K1}}{R_{f2}}\right). \tag{5b}$$

The voltage gain in Fig. 1(a) with global feedback by inspection is then

$$A_{VSF} = \frac{V_{\text{in}}}{V_S}\frac{V_{\text{out}}}{V_{\text{in}}} = \frac{R_{\text{in}}}{R_{\text{in}} + R_S} A_V \tag{5c}$$

where R_{in} is the input resistance of the Kukielka amplifier with global feedback [see Fig. 1(a)]. The formula of R_{in} will be discussed shortly. When the input terminal impedance is matched to R_S, if R_{f2} is much larger than R_{K1}, then

$$A_{VSF} \approx \frac{1}{2} A_V \approx \frac{1}{2} G_{m1} R_{f2} \tag{5d}$$

The current gain $I_{\text{out}}/I_{\text{in}}$ of the A circuit shown in Fig. 1(c) can be easily determined to be

$$A_I = (R_{f1} + R_{e2}) \times G_{m1} \times \frac{R_{f2} + R_{cc} // R_L}{1 + G_{m2}(R_{cc} // R_L)} \times G_{m2}. \tag{6a}$$

Note that the feedback factor $\beta_I = R_{e2}/(R_{f1}+R_{e2})$ and hence $R_{\rm in} = (R_{f1} + R_{e2})/(1 + A_I\beta_I)$ can be obtained easily according to the traditional shunt-series feedback theory.

Finally, the current gain $I_{\rm out}/I_S$ of the A circuit shown in Fig. 1(c) is given by

$$A_{IS} = \frac{I_{\rm out}}{I_S} = \frac{I_{\rm out}}{I_{\rm in}}\frac{I_{\rm in}}{I_S} = A_I\frac{R_S}{R_S + R_{f1} + R_{e2}}. \qquad (6b)$$

As mentioned before, the input resistance is $R_{\rm in} = (R_{f1} + R_{e2})/(1+A_I\beta_I)$ and hence the loop gain T of this shunt-series feedback amplifier can be represented as

$$T = A_{IS}\times\beta_I = \frac{A_I\times\beta_I}{1+(1+A_I\beta_I)\dfrac{R_{\rm in}}{R_s}}. \qquad (7a)$$

For matching $R_{\rm in} = R_s$, the loop gain T becomes

$$T = A_{IS}\times\beta_I = \frac{A_I\times\beta_I}{1+(1+A_I\beta_I)}. \qquad (7b)$$

Clearly, from the above expression, the loop gain T of the Kukielka amplifier is smaller than unity if input is matched. It is the *intrinsic* characteristic of this amplifier. This small loop gain explains why this configuration tends to give an overdamped response [2]. Since $T < 1$

$$\begin{aligned} Q =& \frac{\sqrt{(1+T)\omega_{p1}\omega_{p2}}}{\omega_{p1}+\omega_{p2}} \\ <& \frac{\sqrt{2}\sqrt{\omega_{p1}\omega_{p2}}}{\omega_{p1}+\omega_{p2}} \\ \le& \frac{1}{\sqrt{2}}. \end{aligned}$$

The last equality holds only if $\omega_{p1} = \omega_{p2}$. Thus, because of the low loop gain, it is necessary to design the two open-loop pole positions to be nearly equal and the loop gain as close to 1 as possible, so that the maximally flat condition ($Q = 1/\sqrt{2} = 0.707$) can be approached. Capacitors can be added in parallel to R_{e1} and R_{e2} to introduce peaking, which compensates for the overdamped characteristic of this configuration.

The dc transimpedance gain AZ_{21} by definition is the output voltage (with open load $R_L = \infty$) divided by an ideal current source with $R_S = \infty$, and hence can be easily shown to be

$$AZ_{21} = \frac{A_I}{1 + A_I\cdot\beta_I}\times(R_{f2}//R_{CC}). \qquad (7c)$$

C. Input and Output Resistances

By inspection of Fig. 1(c), the input resistance $R_{\rm inA}$ of the A circuit is $R_{f1} + R_{e2}$. From the results of the shunt-series feedback theory, the input resistance with feedback is given by

$$R_{\rm in} = \frac{R_{f1}+R_{e2}}{1+A_I\beta_I} = \frac{R_{f1}+R_{e2}}{1+G_{m1}\dfrac{R_{f2}+R_{cc}//R_L}{1+G_{m2}(R_{cc}//R_L)}G_{m2}R_{e2}}. \qquad (8a)$$

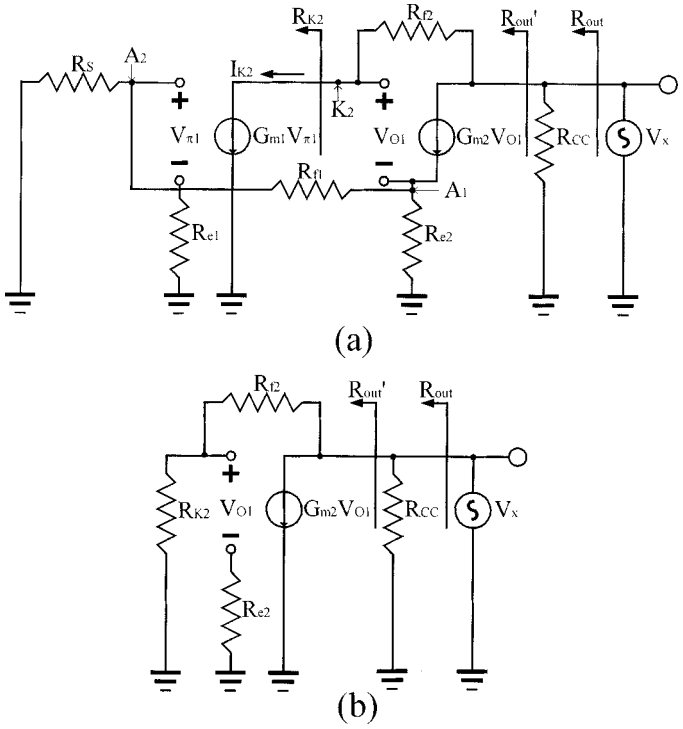

Fig. 2. Circuit diagram for the calculation of the output resistance. (a) The ac equivalent circuit. (b) Simplified schematic.

If $G_{m2}(R_{cc}//R_L) \gg 1$, $R_{f2} \gg R_{cc}//R_L$ and $R_{cc} \gg R_L$, $R_{\rm in}$ can be reduced to

$$R_{\rm in} \approx \frac{R_{f1}+R_{e2}}{1+G_{m1}R_{f2}\dfrac{R_{e2}}{R_L}} = \frac{R_{f1}+R_{e2}}{1+A_V\beta_V} \qquad (8b)$$

where β_V is defined as R_{e2}/R_L. According to Fig. 1(a), β_V has the physical meaning that a portion $R_{e2}/R_L(\beta_V)$ of the output voltage is fed back to the input through resistors R_{f1}, assuming the voltage drop across R_{f1} is negligible. It is interesting to note that $A_I\beta_I$ is approximately equal to $A_V\beta_V$. As we well see, this equality is especially useful when one is designing a voltage amplifier rather than a current amplifier.

As for output resistance, unfortunately, the traditional shunt-series feedback theory cannot give the output resistance at *collector node* that we want. It only provides the output resistance seen between the emitter of Q_2 and resistance R_{e2} [12]. Therefore, we have to derive the output resistance directly from the Kukielka amplifier itself. The circuit diagram for the calculation of output resistance is shown in Fig. 2. When a test voltage V_x is applied to the collector node of Q_2, a voltage of $V_{\rm A1} = G_{m2}V_{O1}R_{e2}$ at A_1 is across the resistor R_{e2}, assuming that the current flowing through the feedback resistor R_{f1} is small. Hence, a voltage of $V_{\rm A2} = G_{m2}V_{O1}R_{e2}R_S/(R_S + R_{f1})$ appears at A_2 and a current I_{K2} of $G_{m1}G_{m2}V_{O1}R_{e2}R_S/(R_S + R_{f1})$ is induced at the collector of Q_1. As a result, the resistance looking into the collector of Q_1, represented by R_{K2}, can be obtained:

$$R_{K2} = \frac{V_{O1}}{I_{K2}} = \frac{R_s + R_{f1}}{R_sG_{m1}G_{m2}R_{e2}}. \qquad (9a)$$

The circuit in Fig. 2(a) then can be simplified to the one shown in Fig. 2(b). From this circuit, the impedance R'_{out} can be easily shown to be $R'_{\text{out}} = (R_{f2} + R_{K2})/(1 + G_{m2}R_{K2})$, and therefore the output resistance is given by

$$R_{\text{out}} = R'_{\text{out}} // R_{cc} = \frac{R_{f2} + R_{K2}}{1 + G_{m2}R_{K2}} // R_{cc}. \tag{9b}$$

Under the assumption that R_{cc} is very large, $R_{f1} \gg R_{e2}$, $A_V\beta_V = G_{m1}R_{f2}R_{e2}/R_L$, and (9b) equals R_S, the output impedance can be rewritten as

$$R_{\text{out}} = \frac{A_V\beta_V R_L + \left(\frac{1}{G_{m2}}\right)(2 + A_V\beta_V)}{\frac{(A_V\beta_V R_L)}{R_{f2}} + 2 + A_V\beta_V}. \tag{9c}$$

D. Frequency Responses of S_{21}, S_{11}, S_{22}, S_{12}, Z_{21}, Z_T

Once the two poles and dc or midband gain are known, the frequency response of $S_{21} = 2\times$ (voltage gain) can be determined easily. However, the traditional theory on frequency response does not provide a general way to determine the frequency responses of input and output return losses, i.e., $|S_{11}|$ and $|S_{22}|$. Here, the determination of the frequency responses of input and output return losses from the poles of voltage gain is proposed. S_{11} is given by

$$S_{11} = \frac{Z_{\text{in}} - R_S}{Z_{\text{in}} + R_S} \tag{10a}$$

where Z_{in} is the input impedance of the amplifier. By definition, the poles of S_{11} are the roots of $Z_{\text{in}} + R_S = 0$. It is known that the poles of all S parameters are the same [13] and hence $Z_{\text{in}} + R_S = 0$ is equivalent to the characteristic (1) for the closed-loop poles of voltage gain. The zeros of S_{11} are the roots of $Z_{\text{in}} - R_S = 0$. This zero equation can be viewed as the transformation of the pole equation $Z_{\text{in}} + R_S = 0$ with R_S replaced by $-R_S$. That is to say, the zero equation of S_{11} can be obtained easily by replacing R_S in (1) with $-R_S$. In other words, the zeros of S_{11}, ω_{Z1} and ω_{Z2} can be obtained by the replacing R_S in the expressions of the poles $P1$ and $P2$ (or ω_{P1} and ω_{P2}) with $-R_S$. At dc frequency, $S_{11} = (R_{\text{in}} - R_S)/(R_{\text{in}} + R_S)$ and therefore S_{11} can be written as follows for all frequencies:

$$S_{11} = \frac{Z_{\text{in}} - R_S}{Z_{\text{in}} + R_S} = \frac{R_{\text{in}} - R_S}{R_{\text{in}} + R_S} \cdot \frac{\left(1 + \frac{s}{\omega_{Z1}}\right)\left(1 + \frac{s}{\omega_{Z2}}\right)}{\left(1 + \frac{s}{P_1}\right)\left(1 + \frac{s}{P_2}\right)}. \tag{10b}$$

By similar arguments, S_{22} can be given by

$$S_{22} = \frac{Z_{\text{out}} - R_L}{Z_{\text{out}} + R_L} = \frac{R_{\text{out}} - R_L}{R_{\text{out}} + R_L} \cdot \frac{\left(1 + \frac{s}{\omega_{Z3}}\right)\left(1 + \frac{s}{\omega_{Z4}}\right)}{\left(1 + \frac{s}{P_1}\right)\left(1 + \frac{s}{P_2}\right)}. \tag{10c}$$

ω_{Z3} and ω_{Z4} are the zeros of S_{22} and are obtained by replacing R_L in the expressions of the poles P_1 and P_2 (or ω_{P1} and ω_{P2}) with $-R_L$.

S_{12} is the reverse voltage gain, which can be found easily once R_{out} is known:

$$S_{12} = 2\left\{\left[(1 + G_{m2}R_{e1})\frac{R_S + R_{f1}}{G_{m2}R_{e2}R_S} + R_{f2}G_{m1}\right] \cdot \left(1 + \frac{R_L}{R_{CC}}\right) + G_{m2}R_L\frac{R_S + R_{f1}}{G_{m2}R_{e2}R_S} + G_{m1}R_L\right\}^{-1} \cdot \frac{\left(1 + \frac{s}{\omega_{z5}}\right)}{\left(1 + \frac{s}{P_1}\right)\left(1 + \frac{s}{P_2}\right)} \tag{10d}$$

where $\omega_{z5} = 1/(C_{\pi 1}R_{e1})$ is the zero caused by $C_{\pi 1}$ and R_{e1}.

The transimpedance Z_{21} *with open load* can be given by

$$Z_{21} = \frac{A_I}{1 + A_I \cdot \beta_I} \times (R_{F2} // R_{CC}) \frac{1}{\left(1 + \frac{s}{P'_1}\right)\left(1 + \frac{s}{P'_2}\right)} \tag{10e}$$

where P'_1 and P'_2 are the two poles given by (2) but with $R_L = R_S = \infty$.

Finally, the transimpedance Z_T with 50-Ω load is calculated according to the following widely used formula:

$$Z_T = \frac{S_{21}}{1 - S_{11}} \cdot 50. \tag{10f}$$

E. Design Equations

Armed with the expressions for poles, voltage gain, current gain, and input and output resistances, we are now ready to derive some useful design equations. Under the assumptions that $G_{m2}R_L \gg 1$, $R_{e1} \ll R_S$, and $\omega_{T1} = \omega_{T2}$, the condition that $\omega_{P1} = \omega_{P2}$ reduces to

$$R_{f2} = G_{m1}(R_S + R_{e1})(R_{cc} // R_L) \approx G_{m1}R_S(R_{cc} // R_L). \tag{11a}$$

The combination of (11a) and (5d) yields the following first-order design equations:

$$R_{f2} = \sqrt{2A_{VSF}R_S\,(R_L // R_{cc})} \tag{11b}$$

$$R_{e1} = \frac{R_s \times (R_{cc} // R_L)}{R_{f2}} - \frac{1}{g_{m1}}. \tag{11c}$$

g_{m1} is dependent on I_{c1}, which is decided by the consideration of power consumption and noise figure. Similar design equations (11a)–(11c) have also been derived previously by Hull and Meyer [2] from the configuration consisting of two local shunt–shunt feedback amplifiers. According to (8a) and (8b), R_{f1} is given by

$$R_{f1} \approx (1 + A_I\beta_I)R_S = (1 + A_V\beta_V)R_S. \tag{11d}$$

The β_V (or R_{e2}) remains to be determined in order to find the value of R_{f1}. Usually, a large R_{f1} is desirable from the requirement of a low noise figure, which means that a large $A_I\beta_I$ or $A_V\beta_V$ is favorable. R_{e2} can be decided by the output matching

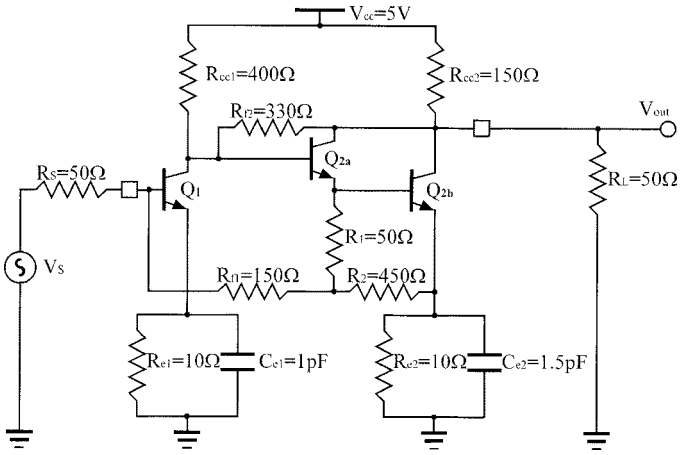

Fig. 3. Schematic of the InGaP–GaAs HBT matched impedance wide-band amplifier with Darlington configuration.

condition. By setting R_{out} of (9c) equal to R_L, the following equation is obtained:

$$R_{\text{out}} = \frac{A_V\beta_V R_L + \left(\frac{1}{G_{m2}}\right)(2 + A_V\beta_V)}{\frac{A_V\beta_V R_L}{R_{f2}} + (2 + A_V\beta_V)} = R_L. \quad (12a)$$

From the above expression, the value of R_{e2}, in general, can be obtained easily.

$$R_{e2} = \frac{R_L\left(\frac{A_V\beta_V R_L}{R_{f2}} + 2\right)}{2 + A_V\beta_V} - \frac{1}{g_{m2}}. \quad (12b)$$

R_{cc} is determined by the dc bias point, which should be around 1/3 of the supply voltage [12]. The bandwidth can be estimated to be $1.414\,\omega_{p1}$ or $1.414\,\omega_{p2}$, assuming maximum flat condition.

III. Circuit Implementation and Measured Results

The schematic of the InGaP–GaAs HBT wide-band amplifier is shown in Fig. 3. Note that the second stage is replaced with the compound transistor, which has a resistive Darlington configuration consisting of Q_{2a} and Q_{2b}. The primary motive for use of the compound transistor is to achieve a higher gain–bandwidth product. The effective transconductance of the compound transistor can be expressed as

$$g_{m\text{eff}} = \frac{g_{m2a} + g_{m2a}g_{m2b}\,(R//r_{\pi 2b})}{1 + g_{m2a}\,(R//r_{\pi 2b})} \approx g_{m2b} \quad (13)$$

where g_{m2a} and g_{m2b} are the transconductances of Q_{2a} and Q_{2b}, respectively, R is $R_1 + R_2$, and $r_{\pi 2b}$ is the base–emitter resistance of Q_{2b}. Clearly, the effective transconductance is dominated by the second transistor (Q_{2b}) of the Darlington configuration. It is also known that in ideal conditions, the Darlington configuration appears as a single transistor with twice f_T. Therefore, in designing the Kukielka circuit with the Darlington pair, the transconductance g_{m2} and cut-off frequency ω_{T2} of the second stage discussed in the previous section may be replaced by $g_{m\text{eff}}$ and $2\omega_{T2b}$. Going through the design procedure described in the previous section, and after some fine tunings, circuit parameters were obtained as indicated in Fig. 3.

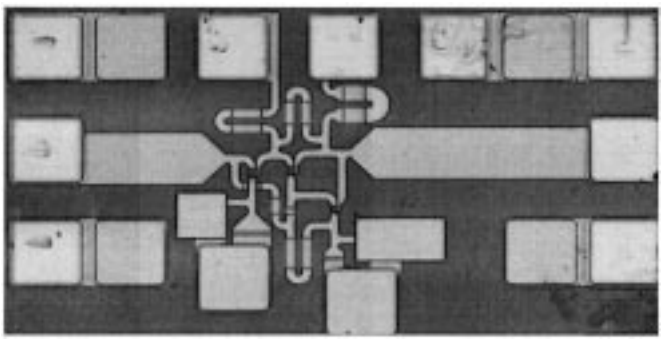

Fig. 4. Die photograph of the InGaP–GaAs HBT matched impedance amplifier. The chip size is only 450 μm × 500 μm excluding the testing patterns.

Note that capacitors were added in parallel to R_{e1} and R_{e2} to introduce peaking for the compensation of the intrinsic overdamped characteristic of the Kukielka amplifier. The peaking capacitors will change the input and output impedance calculations given previously. Therefore, care must be taken with this technique because it will have a detrimental effect on the large signal response (often introducing ringing) and the small-signal group delay.

The wideband amplifier was fabricated with InGaP–GaAs HBT process provided by the commercial foundry of GCS. InGaP–GaAs HBT technology has been chosen because of its higher uniformity [6]–[9], higher reliability [10], and lower $1/f$ noise [14], as compared with the traditional AlGaAs–GaAs HBT process. The device sizes of Q_1, Q_{2a}, and Q_{2b} are 1.4 μm × 9 μm, 1.4 μm × 6 μm, and 1.4 μm × 9 μm, respectively, while the bias currents for the transistors are 4.8, 2.9, and 11.5 mA, respectively. These HBTs have the following device parameters.

$$\begin{aligned} f_{T1} =& 40\text{ GHz}, C_{jc1} = 30\text{ fF}, C_{js1} = 0\text{ fF}, \\ & r_{b1} = 28\,\Omega, g_{m1} = 187\text{ mS} \\ f_{T2a} =& 35\text{ GHz}, C_{jc2a} = 45\text{ fF}, C_{js2a} = 0\text{ fF}, \\ & r_{b2a} = 15\,\Omega, g_{m2a} = 109\text{ mS} \\ f_{T2b} =& 36\text{ GHz}, C_{jc2b} = 45\text{ fF}, C_{js2b} = 0\text{ fF}, \\ & r_{b2b} = 10\,\Omega, g_{m2b} = 363\text{ mS}. \end{aligned}$$

Computer simulations were done by HP Series IV high-frequency circuit design tools. Since this circuit is high frequency in nature, circuit simulations with and without the transmission-line model (TLM) were compared. In order to reduce the chip area and reflections of waves, meandering shapes of resistors were carefully laid out. Direct cascade probable coplanar wave-guide patterns were also laid out for ease of microwave testing. The die photograph of the finished circuit is shown in Fig. 4. Note that the circuit (excluding the patterns for testing) only occupies a very small area of 450 μm × 500 μm because no inductor was used. This is one advantage of the resistive feedback amplifier.

An HP8510 network analyzer in conjunction with the cascade probe station was used to measure the characteristics of this wideband amplifier. The measured and simulated results are shown in Fig. 5(a)–(f) for $|S_{21}|$, $|S_{11}|$, $|S_{22}|$, $|S_{12}|$, $|Z_{21}|$

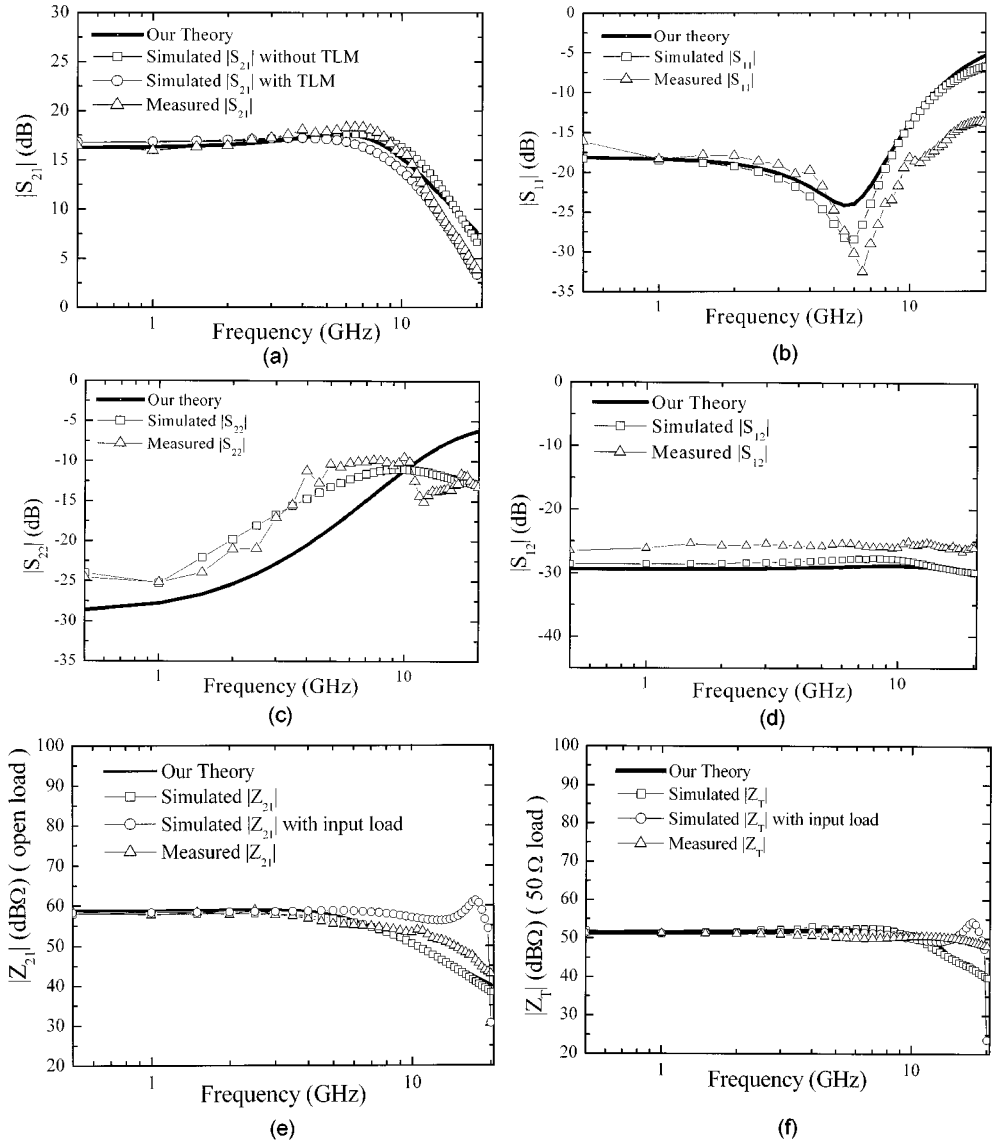

Fig. 5. Simulated and measured S parameters, transimpedance Z_{21} with output open load, and transimpedance Z_T with output 50-Ω load. (a) $|S_{21}|$ simulated results with and without transmission-line effect are both shown. (b) $|S_{11}|$. (c) $|S_{22}|$. (d) $|S_{12}|$. (e) $|Z_{21}|$. (f) $|Z_T|$.

(open load tranimpedance), $|Z_T|$ (50-Ω load transimpedance), respectively. The measured S_{21} exhibited a flat response with a 3-dB bandwidth of 11.6 GHz, and in-band return loss $|S_{11}|$ and $|S_{22}|$ were less than -10 dB. Note that at higher frequencies ($>$10 GHz), the simulated $|S_{21}|$ with TLM agreed better with the measured $|S_{21}|$ as compared with the simulated $|S_{21}|$ without TLM. This indicates that the transmission-line effect cannot be ignored when the frequency is higher than 10 GHz. The predicted $|S_{21}|$ at low frequency by the method we proposed is 17.7 dB, in good agreement with the simulated $|S_{21}|$ of 17 dB and the measured $|S_{21}|$ of 16 dB. The simulated $|S_{11}|$ and $|S_{22}|$ also agreed well with the measured values as shown in Fig. 6(b) and (c), respectively. Also shown are the calculated values of frequency responses from our pole and zero theory for $|S_{21}|$, $|S_{11}|$, $|S_{22}|$, $|S_{12}|$, $|Z_{21}|$, and $|Z_T|$. Reasonably good agreement with the experimental results is found. The predicted bandwidth is 11.4 GHz, which is comparable to the simulated result with TLM of 11.4 GHz and the measured result of

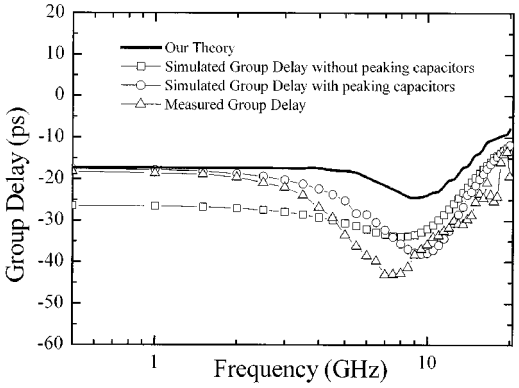

Fig. 6. Simulated and measured group delay response with and without peaking capacitors.

11.6 GHz. The calculated values of $R_{\rm in}$ and $R_{\rm out}$ by our theory are 37.8 and 49.2 Ω, respectively, which are in good agreement

with the simulation results of 37.8 and 57 Ω at low frequency. Also shown in Fig. 5(e) and (f) are the transimpedances calculated with an assumed photodetector capacitive load (100 fF) and wire-bond interconnect inductance (1 nH) [15]. Clearly, this degrades the effective transimpedance, and therefore its influence must be considered carefully in the circuit design. The group delay response with all these feedback loops is shown in Fig. 6 and is compared to that without peaking capacitors. As can be seen, the peaking technique has a detrimental effect on group delay.

IV. Conclusion

The methodology for the analysis and design of a matched-impedance wideband amplifier with multiple feedback loops was proposed. Expressions for voltage gain, current gain, loop gain, transimpedance gain, bandwidth, input/output resistance, and design equations were derived. A general method for the determination of the frequency responses of input/output return losses from the poles of voltage gain was also presented. The first InGaP–GaAs HBT wide-band amplifier with the Kukielka configuration was designed by the proposed methodology. The experimental results showed that small signal gain of 16 dB and a 3-dB bandwidth of 11.6 GHz with in-band input/output return losses less than 10 dB were obtained. The calculated values of small signal gain, bandwidth, input/output resistance, and frequency responses agreed well with those from experimental results. Thus, the verification of our proposed equations was demonstrated.

References

[1] R. G. Meyer and R. A. Blauschild, "A 4-terminal wide-band monolithic amplifier," *IEEE J. Solid-State Circuits*, vol. SC-16, pp. 634–638, Dec. 1981.

[2] C. D. Hull and G. B. Meyer, "Principles of monolithic wideband feedback amplifier design," *Int. J. High Speed Electron.*, vol. 3, pp. 53–93, Feb. 1992.

[3] I. Kipnis, J. K. Kukielka, J. Wholey, and C. P. Snapp, "Silicon bipolar fixed and variable gain amplifier MMICs for microwave and lightwave applications up to 6 GHz," in *IEEE MTT-S Int. Microwave Symp. Dig.*, vol. 1, June 1989, pp. 109–112.

[4] K. W. Kobayashi and A. K. Oki, "A DC-10 GHz high gain-low noise GaAs HBT direct-coupled amplifier," *IEEE Microwave Guided Wave Lett.*, vol. 5, pp. 308–310, Sept. 1995.

[5] K. W. Kobayashi, L. T. Tran, J. Cowls, T. R. Block, a. K. Oki, and D. C. Streit, "Low dc power high gain-bandwidth product InAlAs/InGaAs–InP HBT direct-coupled amplifiers," in *Proc. IEEE GaAs IC Symp.*, Nov. 1996, pp. 141–144.

[6] T. Lester, M. Svilans, P. Maritan, and H. Postolek, "A manufacturable process for HBT circuits," in *Inst. Phys. Conf. Ser.*, vol. 136, 1993, pp. 449–451.

[7] S. S. Lu and C. C. Huang, "High-current-gain $Ga_{0.51}In_{0.49}P/GaAs$ heterojunction bipolar transistor grown by gas-source molecular beam epitaxy," *IEEE Electron. Device Lett.*, vol. 13, pp. 214–216, Apr. 1992.

[8] Y. S. Lin, T. P. Sun, and S. S. Lu, "$Ga_{0.51}In_{0.49}P/In_{0.15}Ga_{0.85}As/GaAs$ pseudomorphic doped-channel FET with high-current density and high-breakdown voltage," *IEEE Electron. Device Lett.*, vol. 18, pp. 150–153, Apr. 1997.

[9] Y. S. Lin, S. S. Lu, and Y. J. Wang, "High-performance $Ga_{0.51}In_{0.49}P/GaAs$ airbridge gate MISFETs grown by gas-source MBE," *IEEE Trans. Electron Devices*, vol. 44, pp. 921–929, June 1997.

[10] H. Willemsen and D. Nicholson, "GaAs ICs in commercial OC-192 equipment," in *Proc. IEEE GaAs IC Symp.*, vol. 1, Nov. 1996, pp. 10–13.

[11] F. T. Chien and Y. J. Chan, "Bandwidth enhancement of transimpedance amplifier by a capacitive-peaking design," *IEEE J. Solid-State Circuits*, vol. 34, pp. 1167–1170, Aug. 1999.

[12] A. S. Sedra and K. C. Smith, *Microelectronic Circuits*, 4 ed. New York: Oxford Univ. Press, 1998.

[13] S. S. Lu, C. C. Meng, T. W. Chen, and H. C. Chen, "A novel interpretation of transistor S-parameters by poles and zeros for RF IC circuit design," *IEEE Trans. Microwave Theory Tech.*, vol. 49, pp. 406–409, Feb. 2001.

[14] B. Pereiaslavets, K. H. Bachem, J. Braunstein, and L. F. Eastman, "GaInP/InGaAs/GaAs graded barrier MODFET grown by OMVPE: design, fabrication and device results," *IEEE Trans. Electron Devices*, vol. 43, pp. 1341–1348, Oct. 1996.

[15] H.-M. Rein, "Si and SiGe bipolar ICs for 10 to 40 Gb/s optical-fiber TDM links," in *High-Speed Circuits for Lightwave Communications*, K.-C. Wang, Ed. Singapore: World Scientific, 1999, p. 368.

Ming-Chou Chiang was born in Taiwan, R.O.C., in 1976. He received the B.S. degree from the Department of Electronics Engineering, National Cheng-Kung University, Tainan, Taiwan, R.O.C., and the M.S. degree from the Institute of Electronics, National Taiwan University, Taipei, Taiwan, R.O.C., in 1999 and 2001, respectively.

In 2002, he joined Winbond Electronics Corporation, Hsinchu, Taiwan, R.O.C., as an RF engineer. His research interests include microwave, RF, and analog mixed-signal integrated circuits design.

Shey-Shi Lu (S'89–M'91–SM'99) received the B.S. degree from National Taiwan University, Taiwan, R.O.C., in 1985, the M.S. degree from Cornell University, Ithaca, NY, in 1988, and the Ph.D. degree from the University of Minnesota at Minneapolis-St. Paul in 1991, all in electrical engineering.

He joined the Department of Electrical Engineering, National Taiwan University, in August 1991 as an Associate Professor and was promoted to full Professor in 1995. His current research interests are in the areas of radio-frequency integrated circuits (RFIC)/monolithic microwave integrated circuits (MMIC) and MEMS-RF electronics.

Chin-Chun Meng received the B.S. degree in electrical engineering from National Taiwan University, Taipei, Taiwan, R.O.C., in 1985 and the Ph.D. degree in electrical engineering from the University of California at Los Angeles in 1992. His doctoral dissertation concerned the first continuous wave (CW) operation of multiquantum-well IMPATT oscillator at 100 GHz.

He joined the Hewlett-Packard Component Group, Santa Clara, CA, in 1993 as a Member of Technical Staff. His area of research and development has included HBT, MESFET, and pseudo-morphic high electron-mobility transistor (pHEMT) for microwave and RF power-amplifier application. He is currently an Associate Professor in the Department of Electrical Engineering, National Chung-Hsing University, Taichung, Taiwan, R.O.C. He is currently involved in development of power devices and circuits for wireless communication. His research and publications are in the field of microwave circuits and semiconductor devices.

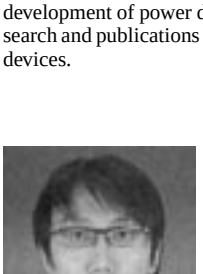

Shih-An Yu was born in Taipei, Taiwan, R.O.C., in 1976. He received the B.S. and M.S. degrees in electrical engineering from National Taiwan University, Taipei, Taiwan, R.O.C., in 1999 and 2001, respectively. He is currently a student in the Institute of Electrical Engineering of National Taiwan University, in the field of communication and RF CMOS circuits.

His current research interests are in high-speed wireless LAN and mobile applications.

Shih-Cheng Yang was born in Taichung, Taiwan, R.O.C., in 1976. He received the B.S. degree from the Department of Electrical Engineering, National Central University, Chung-Li, Taiwan, R.O.C., in 1997, where he is currently working toward the Ph.D. degree.

His research interests are in the areas of submicron technology, microwave devices, and optoelectronic integrated circuits.

Yi-Jen Chan received the B.S.E.E. degree from National Cheng Kung University, Tainan, Taiwan, R.O.C., the M.S.E.E. degree from National Tsing Hua University, Hsinchu, Taiwan, R.O.C., and the Ph.D. degree in electrical engineering and computer science from the University of Michigan, Ann Arbor, in 1982,1984, and 1992, respectively.

He joined the Department of Electrical Engineering, National Central University, Chungli, Taiwan, R.O.C., as a Faculty Member in 1992. His current research interests include submicron technology, microwave devices, and integrated circuits and optoelectronic integrated circuits.